SUPPORTING INFORMATION

Diradical Character of Neutral Heteroleptic Bis(1,2-dithiolene) Metal Complexes: Case Study of [Pd(Me_2timdt)(mnt)] (Me_2timdt = 1,3-Dimethyl-2,4,5-trithioxoimidazolidine; mnt^{2-} = 1,2-Dicyano-1,2-ethylenedithiolate)

M. Carla Aragoni, [†] *Claudia Caltagirone,* [†] *Vito Lippolis,*[†] *Enrico Podda,*[†] *Alexandra M. Z. Slawin,* [‡] *J. Derek Woollins*[§,‡] *Anna Pintus,** [†] *and Massimiliano Arca**[†]

[†] Dipartimento di Scienze Chimiche e Geologiche, Università degli Studi di Cagliari, S. S. 554 bivio per Sestu, 09042 Monserrato (Cagliari), Italy

E-mail: marca@unica.it

[‡] EaStCHEM School of Chemistry, University of St. Andrews, North Haugh, St. Andrews, Fife, KY16 9ST, UK

[§] Department of Chemistry, Khalifa University, P.O. Box 127788, Abu Dhabi, United Arab Emirates

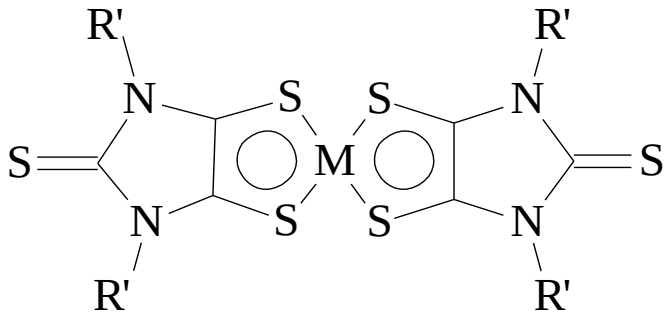

Chart S1. Molecular scheme of neutral [M(R'$_2$timdt)$_2$] bis(1,2-dithiolene) complexes.

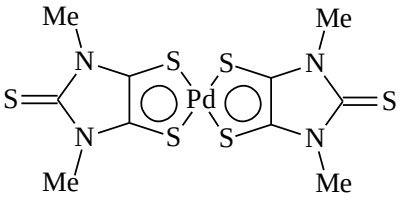

1

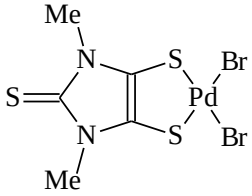

2

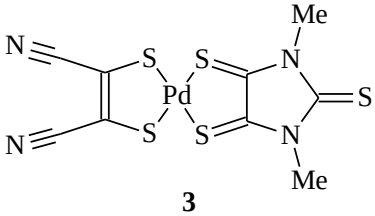

3

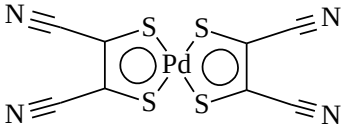

4

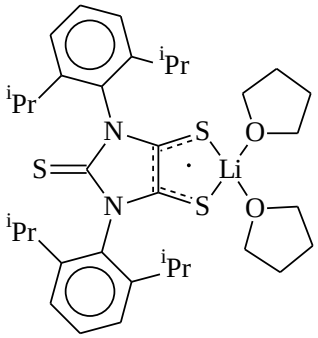

5

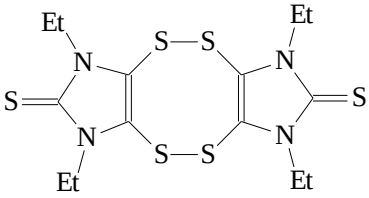

6

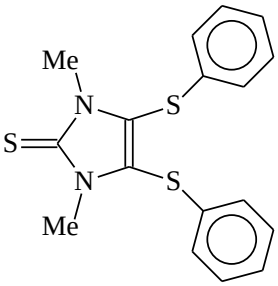

7

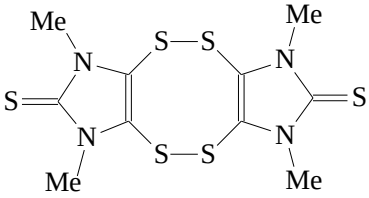

$(Me_2timdt)_2$

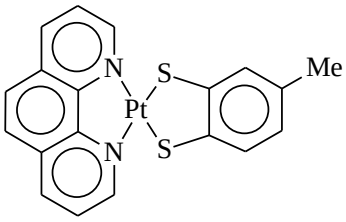

[Pt(phen)(tdt)

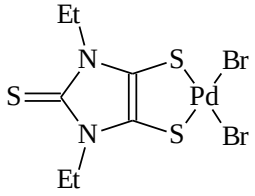

$[Pd(Et_2timdt)Br_2]$

Chart S2. Molecular scheme of compounds **1**–**7**, $(Me_2timdt)_2$, [Pt(phen)(tdt)], and $[Pd(Et_2timdt)Br_2]$. Bis(1,2-dithiolene) Pd complexes **1**–**4** are represented in their neutral forms.

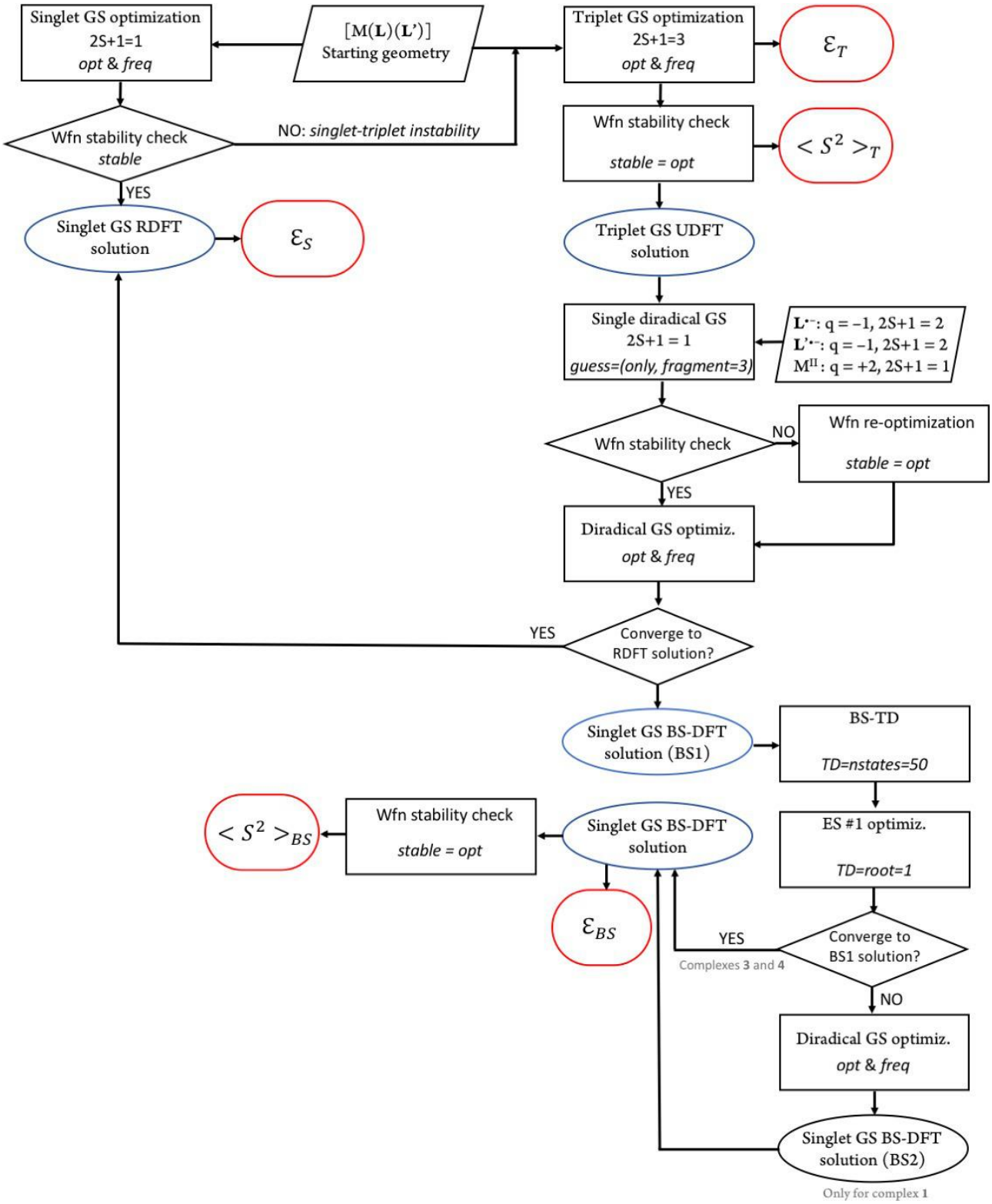

Chart S3. Flowchart representing the calculations for modeling neutral bis(1,2-dithiolene) metal complexes [M(**L**)(**L**')] (M = Ni, Pd) in their triplet ground state, in the closed-shell singlet state, and as antiferromagnetically coupled singlet diradicals in a broken-symmetry (DFT-BS) approach. Each optimized geometry was verified by a vibrational frequency calculation, omitted in the flowchart for the sake of clarity.

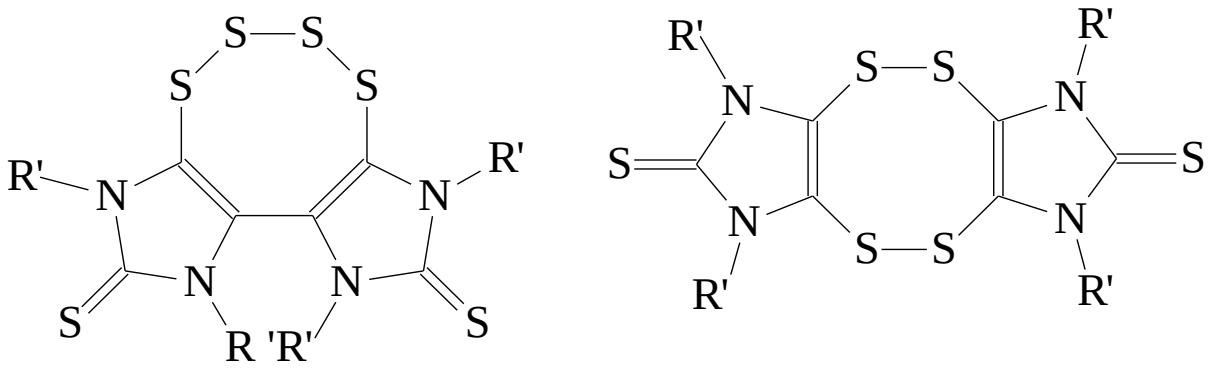

Chart S4. Molecular scheme of tetrasubstituted tetrathiocino derivatives obtained by sulfuration of the corresponding disubstituted imidazolidine-2-thione-4,5-dione.

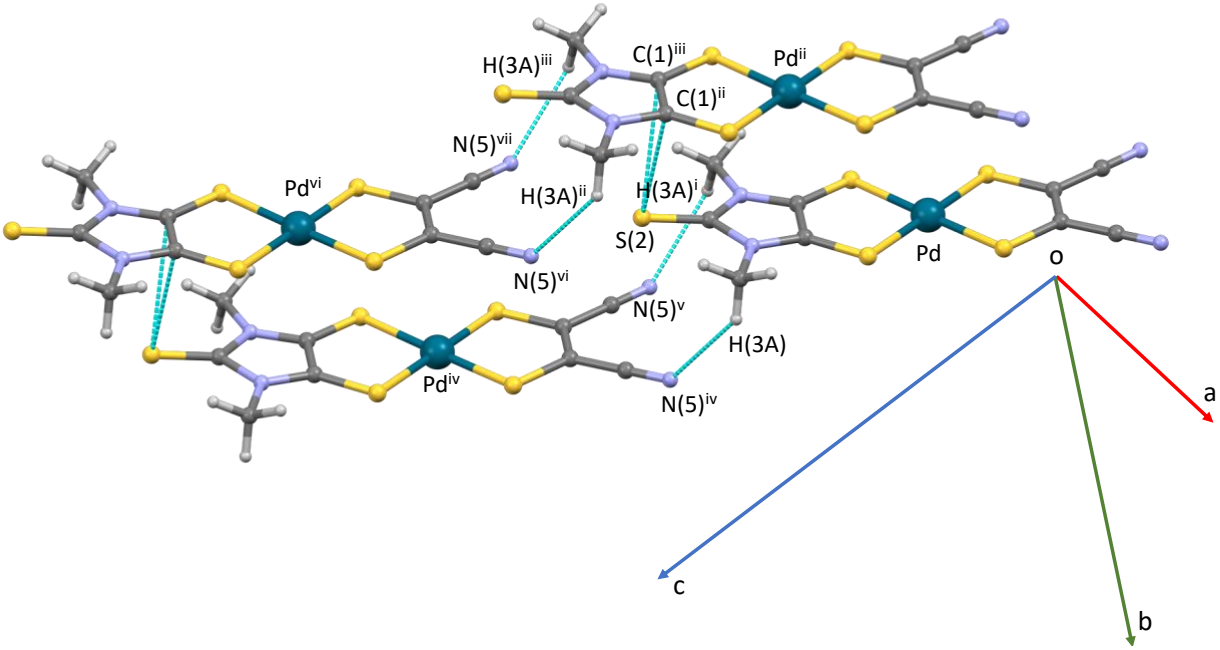

Figure S1. Intermolecular interactions responsible for the packing in compound **3**. Only the atoms involved in the interactions are labelled. S(2)–C(1)$^{ii/iii}$ 3.420, H3A···N(5)$^{iv/v}$ 2.644. Symmetry operations: ^{i} = x, ½-y, z; ^{ii} = -1+x, y, z; ^{iii} =-1+x, ½-y, z; ^{iv} = -1+x, y, 1+z; ^{v} = -1+x, ½-y, 1+z; ^{vi} = -2+x, y, 1+z; ^{vii} = -2+x, ½-y, 1+z.

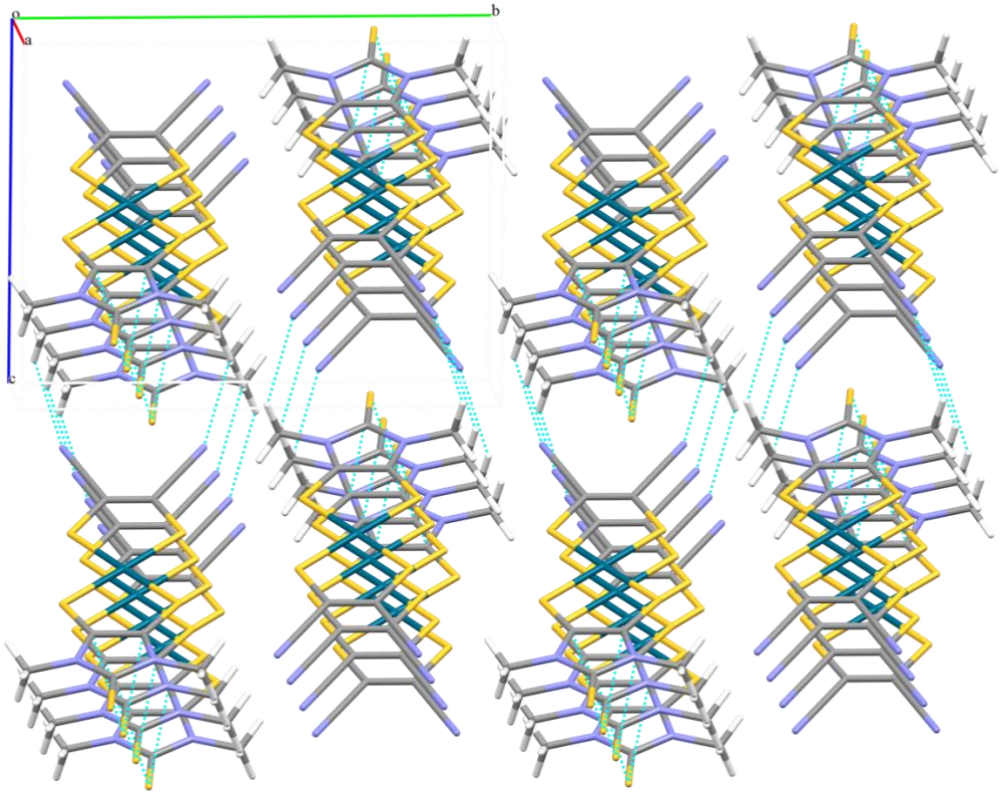

Figure S2. Parallel stacks of neutral molecules of **3** seen along the *a* vector.

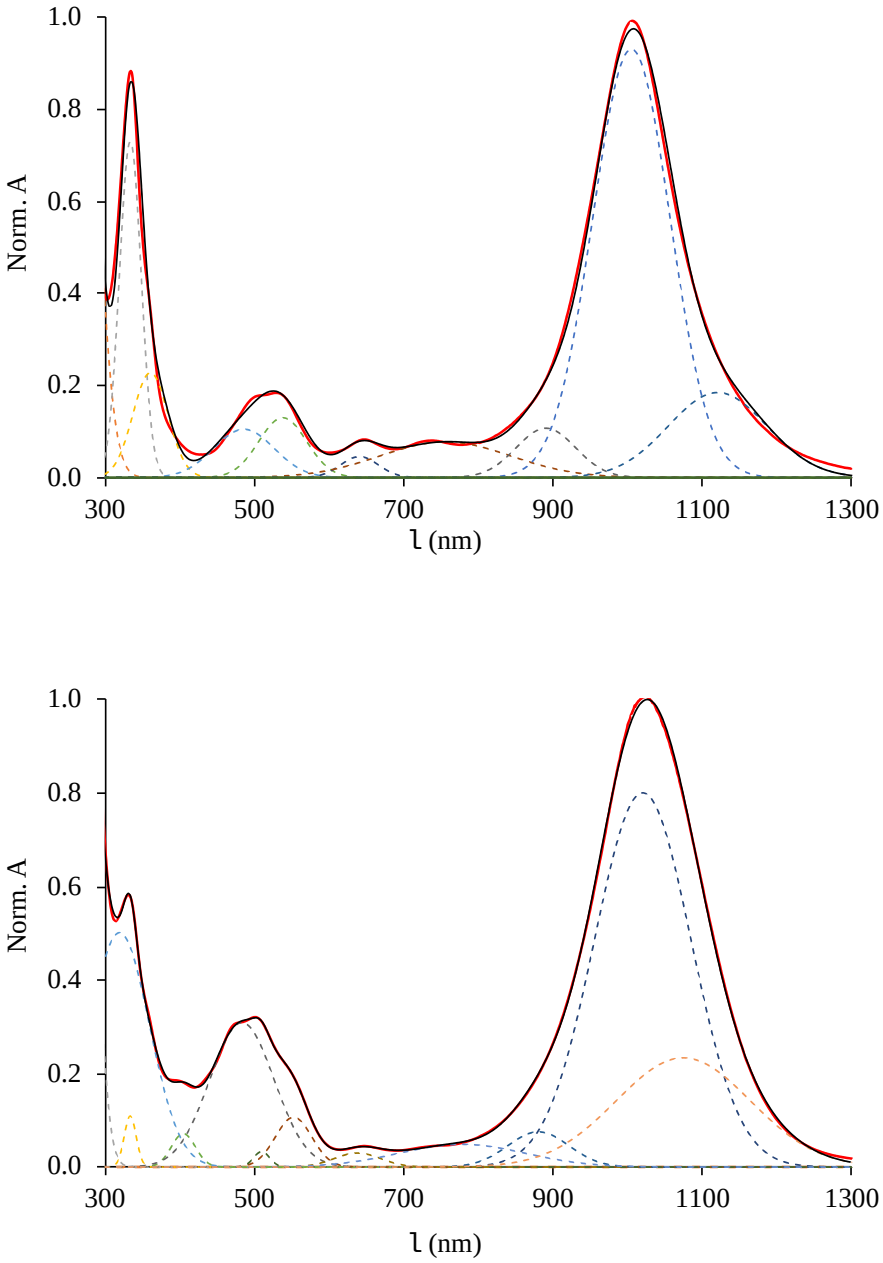

Figure S3. Experimental (red continuous line) normalized UV–vis–NIR absorption spectrum (300–1300 nm) of complex **1** (top) and complex **3** (bottom) in CH_2Cl_2 solution decomposed into Gaussian peaks (dashed line). The spectrum simulated as the sum of the constituent components is reproduced as a black continuous line. Components of the NIR band in complex **1** (top): λ_1 = 1004.8 nm, w_1 = 121.9 nm, integral ratio 74.5%; λ_2 = 890.3 nm, w_2 = 93.5 nm, 6.6%; λ_3 = 1120.2 nm, w_3 = 155.42 nm, 18.9%. Components of the NIR band in complex **3** (bottom): λ_1 = 1020.0 nm, w = 152.3 nm, 68.3% and λ_2 = 1074.2 nm, w_2 = 211.6 nm, 27.6%; λ_3 = 880.3 nm, w_3 = 96.4 nm, 4.1%.

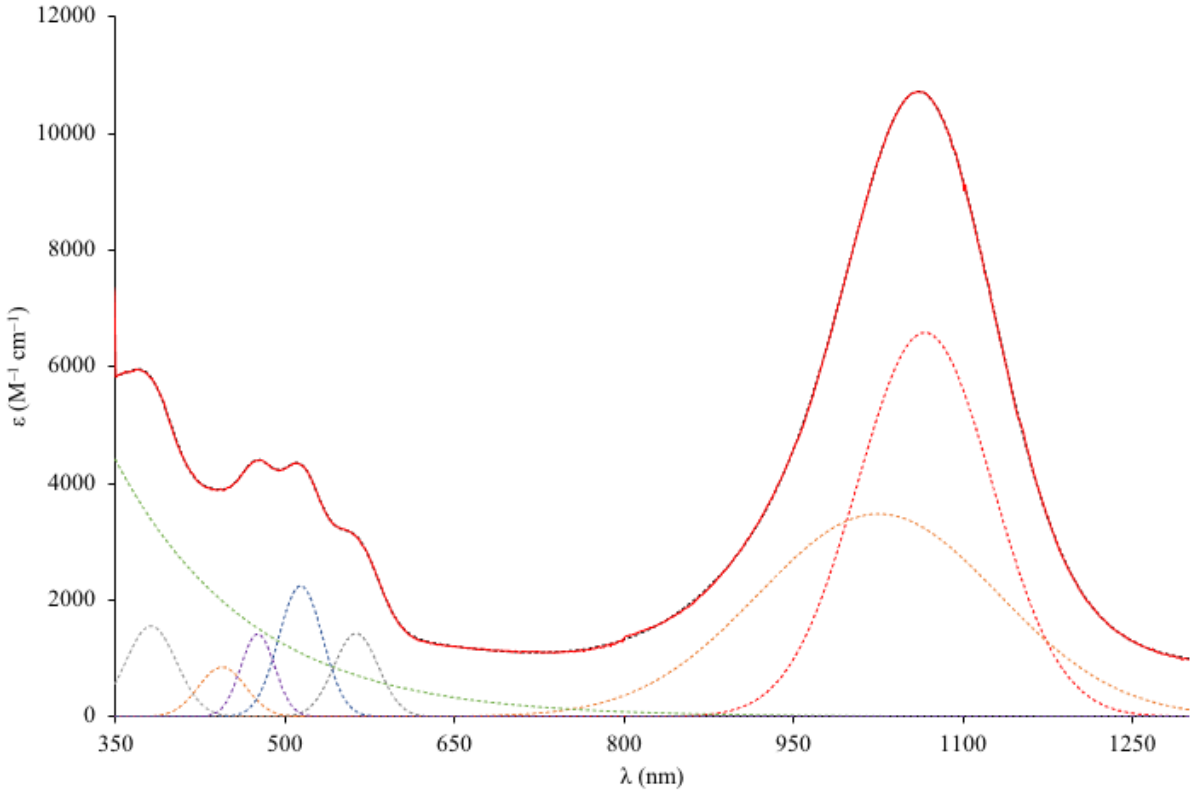

Figure S4. Experimental (red continuous line) UV–vis–NIR absorption spectrum (350–1300 nm) of complex **3** in $CHCl_3$ solution decomposed into Gaussian peaks (dashed line). A broad baseline peak is not depicted. The spectrum simulated as the sum of the constituent components is reproduced as a black continuous line. Components of the NIR band: λ_1 = 1066.2 nm, w_1 = 140.6 nm, 51.6%, λ_2 = 1025.1 nm, w_2 = 249.5 nm, 48.4%.

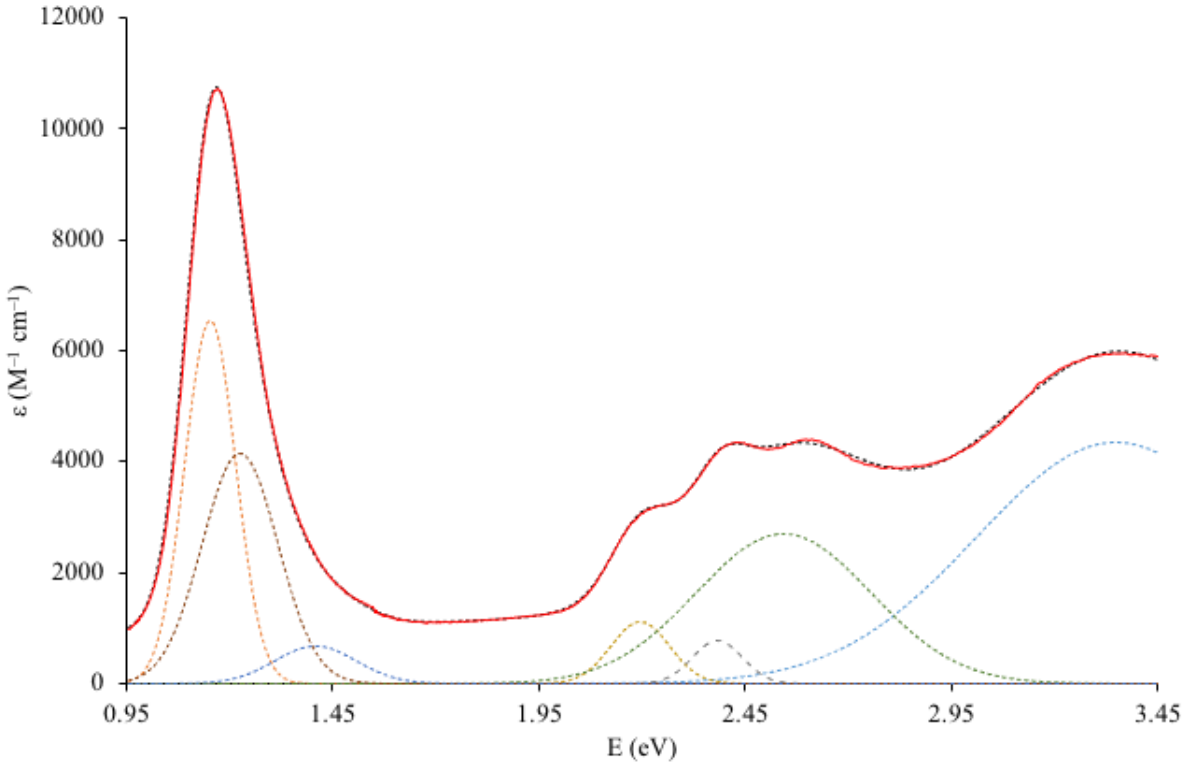

Figure S5. Experimental (red continuous line) UV–vis–NIR absorption spectrum (energy scale 0.95–3.45 eV) of complex **3** in $CHCl_3$ solution decomposed into Gaussian peaks (dashed line). The broad peak mimicking the baseline is not depicted. The spectrum simulated as the sum of the constituent components is reproduced as a black continuous line. Components of the NIR band: E_1 = 1.115 eV, w_1 = 0.145 eV, 47.4%, E_2 = 1.227 eV, w_2 = 0.216 eV, 44.6%; E_3 = 1.410 eV, w_2 = 0.232 eV, 8.0%.

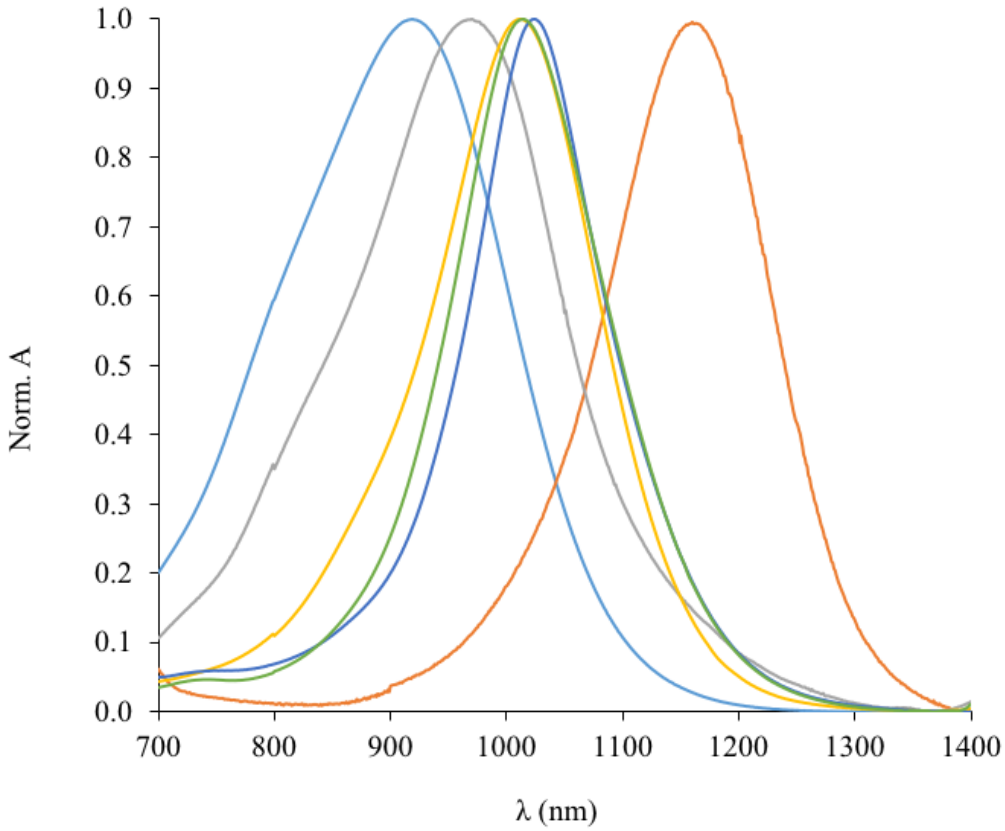

Figure S6. Normalized vis–NIR spectrum (700–1400 nm) recorded for complex **3** in MeCN (cyan), DMF (grey), THF (yellow), CH_2Cl_2 (green), and $CHCl_3$ (orange).

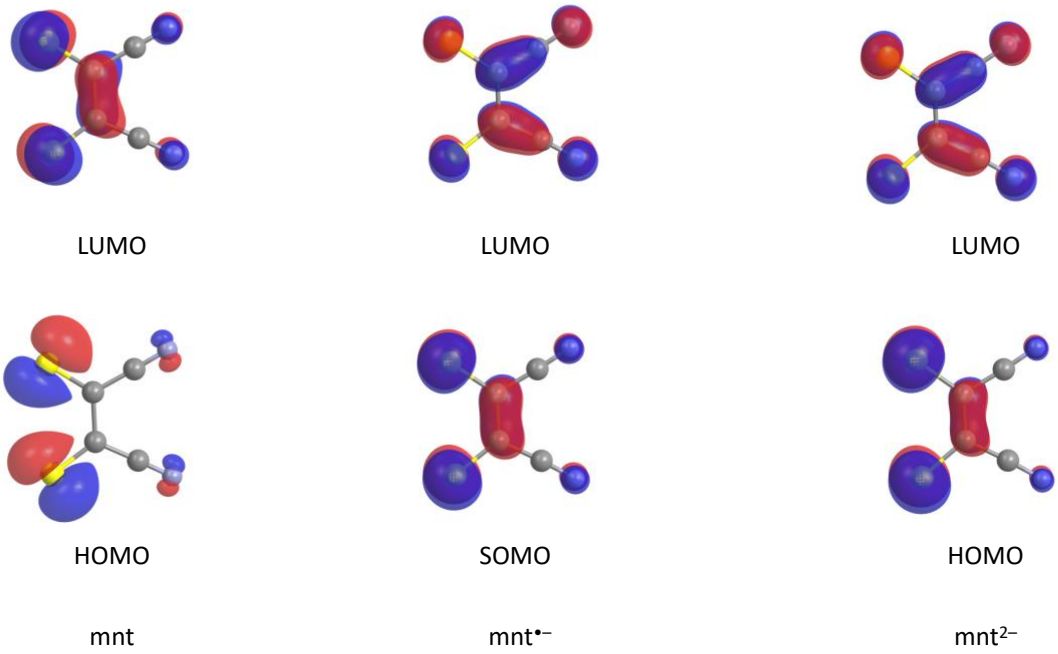

Figure S7. Frontier MO isosurfaces calculated for the free ligand mnt^{q-} (q = 0, 1, 2). Cutoff value = 0.05 |e|.

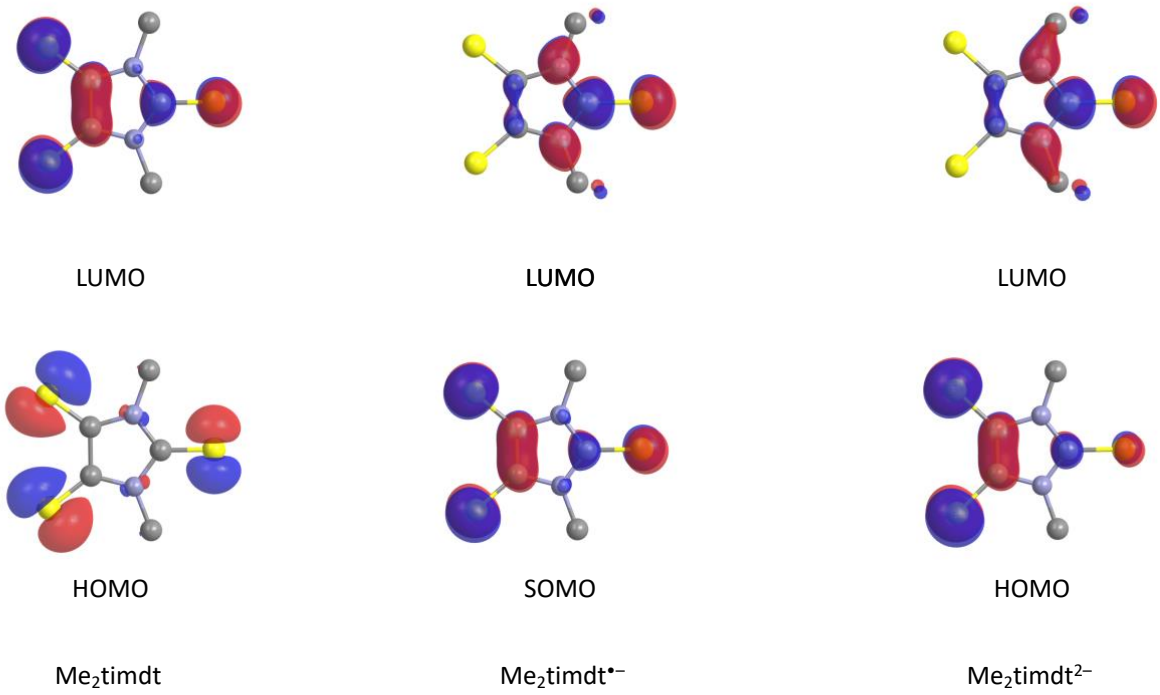

Figure S8. Frontier MO isosurfaces calculated for the free ligand Me_2timdt^{q-} (q = 0, 1, 2). Hydrogen atoms have been omitted for clarity. Cutoff value = 0.05 |e|.

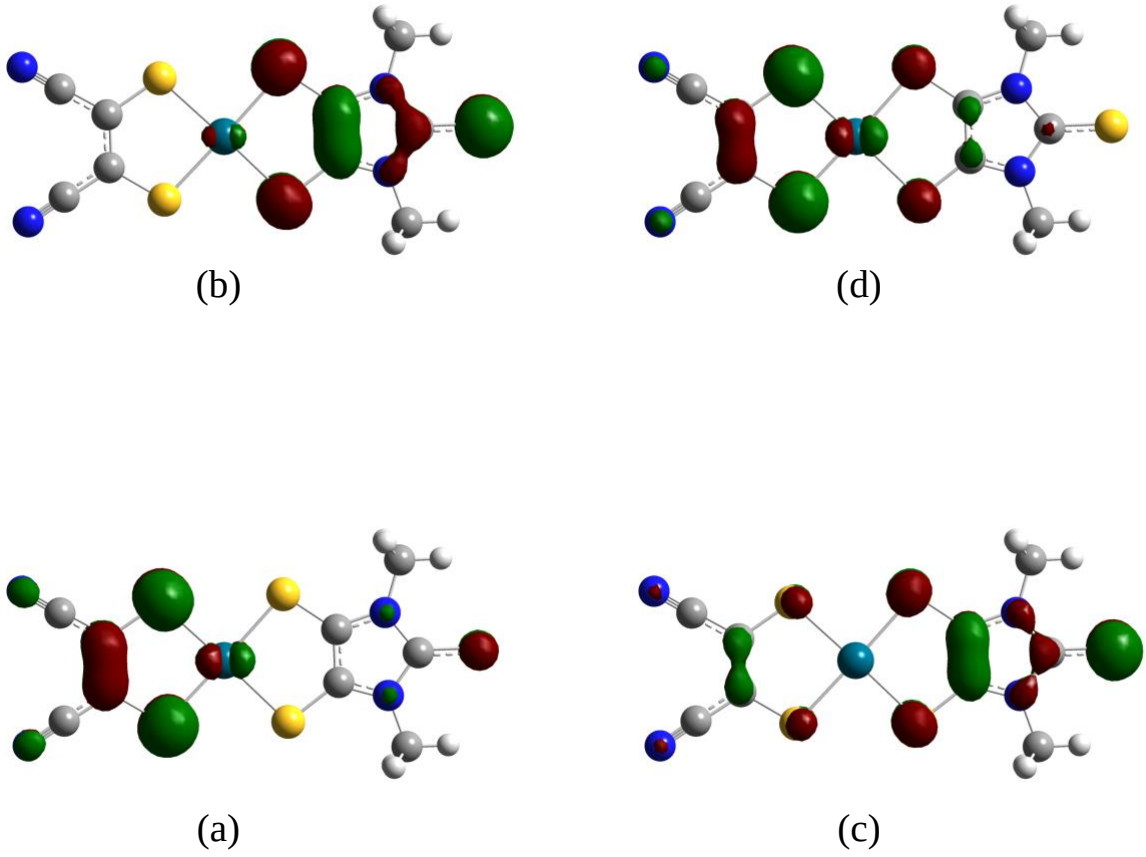

Figure S9. Frontier MOs [α-HOMO (a), α-LUMO (b), β-HOMO (c), and β-LUMO(d)] calculated for complex **3** at DFT-BS level. Cutoff value = 0.05 |e|.

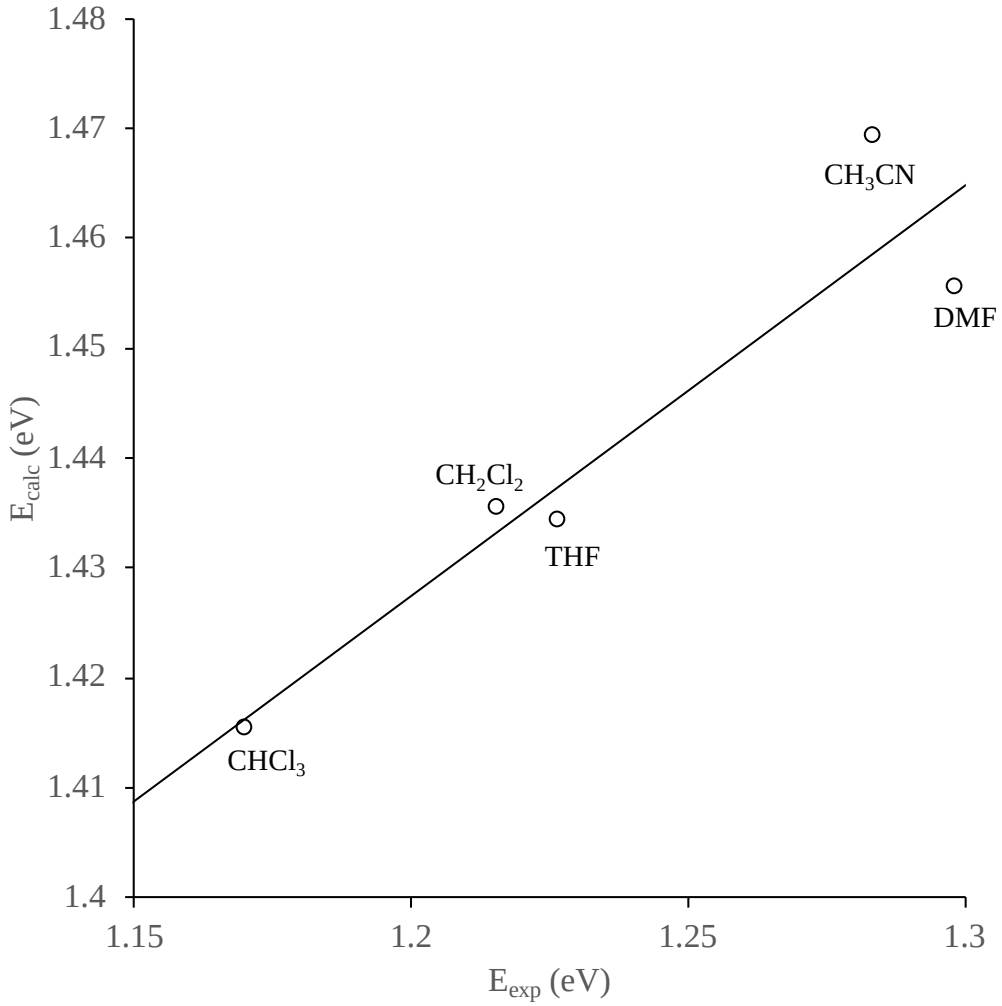

Figure S10. Correlation between NIR-transition energies E_{exp} and the corresponding values E_{calc} calculated for complex **3** at TD-RDFT IEF-PCM level for selected solvents.

Table S1. Crystal data and structure refinement for complex **3**.

Empirical formula	$C_9H_6N_4PdS_5$
Formula weight	436.88
Temperature	93(2) K
Wavelength	0.71073 Å
Crystal system	Monoclinic
Space group	P2(1)/m
Unit cell dimensions	a = 4.924(2) Å α = 90 °.
	b = 13.674(6) Å β = 93.132(13) °.
	c = 10.574(4) Å γ = 90 °.
Volume	710.9(5) $Å^3$
Z	2
Density (calculated)	2.041 Mg/m^3
Absorption coefficient	2.027 mm^{-1}
F(000)	428
Crystal size	0.10 x 0.02 x 0.02 mm^3
θ range for data collection	1.93 to 25.33°.
Index ranges	$-5 \le h \le 4$, $-16 \le k \le 16$, $-12 \le l \le 12$
Reflections collected	4608
Independent reflections	1350 [R(int) = 0.0742]
Completeness to θ = 25.00°	99.7%
Absorption correction	Multiscan
Max. and min. transmission	1.0000 and 0.8420
Refinement method	Full-matrix least-squares on F^2
Data / restraints / parameters	1350 / 0 / 93
Goodness-of-fit on F^2	1.083
Final R indices [I>2sigma(I)]	R1 = 0.0634, wR2 = 0.1306
R indices (all data)	R1 = 0.0938, wR2 = 0.1466
Largest diff. peak and hole	0.915 and –1.029 $e \cdot Å^{-3}$

Table S2. Atomic coordinates (x 10^4) and equivalent isotropic displacement parameters ($Å^2$x 10^3) for complex **3**. U(eq) is defined as one third of the trace of the orthogonalized U^{ij} tensor.

	x	y	z	U(eq)
Pd(1)	7521(2)	2500	5280(1)	32(1)
S(1)	5404(4)	3712(2)	6392(2)	34(1)
C(1)	3614(15)	3032(6)	7345(6)	29(2)
N(1)	1829(12)	3304(5)	8192(6)	29(2)
S(2)	-1715(6)	2500	9760(3)	42(1)
C(2)	590(20)	2500	8748(11)	36(3)
C(3)	1234(17)	4314(6)	8507(8)	41(2)
S(4)	9560(4)	3674(2)	4167(2)	35(1)
C(4)	11337(15)	2999(6)	3110(6)	32(2)
C(5)	12807(17)	3535(6)	2219(8)	34(2)
N(5)	13971(15)	3969(6)	1505(7)	43(2)

Table S3. Bond lengths [Å] and angles [°] for complex **3**.

Pd(1)-S(4)^{i}	2.258(2)
Pd(1)-S(4)	2.258(2)
Pd(1)-S(1)^{i}	2.314(2)
Pd(1)-S(1)	2.314(2)
S(1)-C(1)	1.660(8)
C(1)-N(1)	1.342(9)
C(1)-C(1)^{i}	1.454(16)
N(1)-C(2)	1.401(10)
N(1)-C(3)	1.454(10)
S(2)-C(2)	1.603(13)
C(2)-N(1)^{i}	1.401(9)
C(3)-H(3A)	0.9800
C(3)-H(3B)	0.9800
C(3)-H(3C)	0.9800
S(4)-C(4)	1.724(8)
C(4)-C(4)^{i}	1.364(16)
C(4)-C(5)	1.423(11)
C(5)-N(5)	1.139(10)
S(4)^{i}-Pd(1)-S(4)	90.61(12)
S(4)^{i}-Pd(1)-S(1)^{i}	88.93(8)
S(4)-Pd(1)-S(1)^{i}	179.15(8)
S(4)^{i}-Pd(1)-S(1)	179.15(8)
S(4)-Pd(1)-S(1)	88.92(8)
S(1)^{i}-Pd(1)-S(1)	91.53(12)
C(1)-S(1)-Pd(1)	100.1(3)
N(1)-C(1)-C(1)^{i}	106.1(5)
N(1)-C(1)-S(1)	129.7(6)
C(1)^{i}-C(1)-S(1)	124.1(3)
C(1)-N(1)-C(2)	112.2(7)
C(1)-N(1)-C(3)	124.4(7)
C(2)-N(1)-C(3)	123.5(7)
N(1)-C(2)-N(1)^{i}	103.4(10)
N(1)-C(2)-S(2)	128.3(5)
N(1)^{i}-C(2)-S(2)	128.3(5)
N(1)-C(3)-H(3A)	109.5
N(1)-C(3)-H(3B)	109.5
H(3A)-C(3)-H(3B)	109.5
N(1)-C(3)-H(3C)	109.5
H(3A)-C(3)-H(3C)	109.5
H(3B)-C(3)-H(3C)	109.5
C(4)-S(4)-Pd(1)	102.3(3)
C(4)^{i}-C(4)-C(5)	121.0(5)
C(4)^{i}-C(4)-S(4)	122.4(3)
C(5)-C(4)-S(4)	116.6(6)
N(5)-C(5)-C(4)	179.5(10)

Symmetry transformations used to generate equivalent atoms: ^{i} = x, -y+1/2, z.

Table S4. Anisotropic displacement parameters ($Å^2$ x 10^3) for complex **3**. The anisotropic displacement factor exponent takes the form: $-2\pi^2[h^2 a^{*2}U^{11} + ... + 2 h k a^* b^* U^{12}]$

	U^{11}	U^{22}	U^{33}	U^{23}	U^{13}	U^{12}
Pd(1)	34(1)	35(1)	29(1)	0	5(1)	0
S(1)	36(1)	34(1)	32(1)	-2(1)	7(1)	-2(1)
C(1)	29(4)	39(5)	19(4)	-4(3)	4(3)	2(4)
N(1)	27(3)	29(4)	31(3)	3(3)	4(3)	-1(3)
S(2)	37(2)	52(2)	37(2)	0	10(1)	0
C(2)	30(6)	35(8)	43(7)	0	-3(5)	0
C(3)	39(5)	45(6)	39(5)	-1(4)	10(4)	9(4)
S(4)	40(1)	34(1)	31(1)	-1(1)	9(1)	-1(1)
C(4)	22(4)	49(5)	25(4)	2(3)	9(3)	-8(4)
C(5)	34(5)	27(5)	42(5)	-4(4)	6(4)	-2(4)
N(5)	43(4)	39(5)	48(4)	0(4)	16(4)	-2(4)

Table S5. Hydrogen coordinates (x 10^4) and isotropic displacement parameters ($Å^2$ x 10^3) for complex **3**.

	x	y	z	U(eq)
H(3A)	2544	4541	9174	61
H(3B)	-610	4357	8807	61
H(3C)	1368	4724	7753	61

Table S6. Torsion angles [°] for complex **3**.

S(4)^{i}-Pd(1)-S(1)-C(1)	123(6)
S(4)-Pd(1)-S(1)-C(1)	179.6(2)
S(1)^{i}-Pd(1)-S(1)-C(1)	0.3(3)
Pd(1)-S(1)-C(1)-N(1)	-176.4(6)
Pd(1)-S(1)-C(1)-C(1)^{i}	-0.2(2)
C(1)^{i}-C(1)-N(1)-C(2)	-1.0(6)
S(1)-C(1)-N(1)-C(2)	175.7(6)
C(1)^{i}-C(1)-N(1)-C(3)	178.9(5)
S(1)-C(1)-N(1)-C(3)	-4.5(10)
C(1)-N(1)-C(2)-N(1)^{i}	1.5(10)
C(3)-N(1)-C(2)-N(1)^{i}	-178.3(5)
C(1)-N(1)-C(2)-S(2)	-177.6(7)
C(3)-N(1)-C(2)-S(2)	2.5(12)
S(4)^{i}-Pd(1)-S(4)-C(4)	2.0(3)
S(1)^{i}-Pd(1)-S(4)-C(4)	-55(6)
S(1)-Pd(1)-S(4)-C(4)	-177.3(2)
Pd(1)-S(4)-C(4)-C(4)^{i}	-1.6(2)
Pd(1)-S(4)-C(4)-C(5)	177.9(5)
C(4)^{i} -C(4)-C(5)-N(5)	147(100)
S(4)-C(4)-C(5)-N(5)	-33(100)

Symmetry transformations used to generate equivalent atoms: ^{i} = x, -y+1/2, z.

Table S7. Mulliken contribution (%) of the central metal ion and the mnt and Me_2timdt ligands to the frontier KS-MOs calculated at DFT level for complex **3** (CS GS configuration) in the gas phase and in selected solvents.[a]

		Pd	mnt	Me_2timdt
HOMO (93)	Gas	8	61	31
	$CHCl_3$	9	68	23
	CH_2Cl_2	10	69	21
	THF	10	69	21
	CH_3CN	10	70	20
	DMF	10	70	20
LUMO (94)	Gas	6	24	70
	$CHCl_3$	6	16	78
	CH_2Cl_2	6	14	80
	THF	6	15	80
	CH_3CN	5	13	82
	DMF	5	13	82

[a] IEF-PCM solvation model.

Table S8. Mulliken contribution (%) of the central metal ion and the mnt and Me_2timdt ligands to the frontier KS-MOs calculated at DFT level for complex **3** in the CS and BS description of the GS in the gas phase.

GS	KS-MO	Pd	mnt	Me_2timdt
CS Singlet	HOMO (93)	8	61	31
	LUMO (94)	6	24	70
BS	α-93	9	76	14
	β-93	6	32	63
	α-94	4	5	91
	β-94	10	54	36

Table S9. Transition energy E (cm^{-1} and eV), wavelength λ (nm), oscillator strength f, and one-electron excitation contributions to the NIR transition calculated in the gas phase and at IEF-PCM RDFT level in selected solvents for complex **3**.[a]

	E (cm^{-1})	E (eV)	λ (nm)	f
gas	12010	1.489	832.6	0.315
$CHCl_3$	11416	1.416	876.0	0.385
CH_2Cl_2	11577	1.436	863.8	0.368
THF	11568	1.435	864.4	0.368
CH_3CN	11850	1.469	843.9	0.340
DMF	11739	1.456	851.8	0.356

[a] IEF-PCM solvation model.

Table S10. β components (a.u.), β_{tot} values (a.u. and esu) and dipole moments μ (a.u. and D) calculated for complex **3** in the gas phase, in CH_2Cl_2 and $CHCl_3$.

	Gas (CS)	Gas (BS)	CH_2Cl_2[a]	$CHCl_3$[a]
β_{xxx}	0.00	0.00	0.00	0.00
β_{xxy}	0.00	0.00	0.00	0.00
β_{yxy}	0.00	0.00	0.00	0.00
β_{yyy}	0.00	0.00	0.00	0.00
β_{xxz}	52.44	57.28	102.50	73.96
β_{yxz}	0.00	0.00	0.00	0.00
β_{yyz}	-0.18	-290.02	-76.78	-44.49
β_{zxz}	0.00	0.00	0.00	0.00
β_{zyz}	0.00	0.00	0.00	0.00
β_{zzz}	4301.37	20763.10	55019.10	38215.00
β_{tot} (a.u.)	4353.63	20530.37	55044.82	38244.47
$\beta_{tot} \cdot 10^{-30}$ (esu)	37.62	177.40	475.64	330.47
μ (a.u.)	4.99	4.46	8.02	7.45
μ (Debye)	11.44	11.33	20.39	18.94

[a] IEF-PCM solvation model.